Protein Engineering

DOI: 10.1002/anie.200903075

Protein Scaffold Engineering Towards Tunable Surface Attachment**

Arnon Heyman, Izhar Medalsy, Oron Bet Or, Or Dgany, Maya Gottlieb, Danny Porath, and Oded Shoseyov**

The desire to control, predict, and manipulate protein adsorption to specific surfaces has been the main driving force for intensive research in the past few years directed at gaining a better understanding and control over such protein–surface interactions.[1,2] Controlling the affinity of proteins to surfaces is of great importance for applications such as memory arrays, biosensors, and novel composite materials.[3] The main strategies towards immobilizing proteins are either by surface modifications or through engineering specific surface-binding groups at different locations on the protein structure. The main drawback of the former is the alteration of the bulk chemical surface characteristics and the need of an extensive surface processing, typically involved with multiple steps. The latter strategy typically requires a single step, but is often untunable and frequently results in low surface affinity. Overcoming the need for surface modifications combined with control of the protein surface affinity would enable the exploitation of protein immobilization for new materials and will increase future fabrication throughput.

SP1, a ring-like protein that is highly stable to boiling and protease resistant,[4–7] was recently proposed as a new self-assembled molecular scaffold for nanobiotechnology and biomaterials applications.[8–11] Herein we present a novel strategy to control the interfacial adsorption of SP1 to an unmodified surface with high selectivity and controlled affinity. By genetically fusing specific affinity peptides to retractable N termini, we were able to control the protein surface affinity for the first time by simply changing the solvent conditions.

[*] I. Medalsy,[+] M. Gottlieb, Dr. D. Porath
Physical Chemistry Department and Center for Nanoscience and Nanotechnology, The Hebrew University of Jerusalem
Jerusalem 91904 (Israel)
E-mail: porath@chem.ch.huji.ac.il

A. Heyman,[+] O. Bet Or, Dr. O. Dgany, Prof. O. Shoseyov
The Robert H. Smith Institute of Plant Sciences and Genetics in Agriculture, and the Otto Warburg Minerva Center for Agricultural Biotechnology, Faculty of Agricultural, Food and Environmental Quality Sciences, The Hebrew University of Jerusalem
P.O. Box 12, Rehovot 76100 (Israel)
E-mail: shoseyov@agri.huji.ac.il

[+] These authors contributed equally to this work.

[**] We thank Dr. Igor Brodsky and Dr. Ilan Levy for assistance and discussions, and Eran Zehavy for assistance with the graphics. This research was supported in part by a grant from the BIOMEDNANO STREP project of the European Community and a Trilateral DFG grant CU 44/3-2.

Supporting information for this article is available on the WWW under http://dx.doi.org/10.1002/anie.200903075.

Understanding the dependence of the protein surface affinity on its structure is a key element in engineering a novel surface-binding scaffold. To fully understand the availability of the protein structure to the surface, the protein affinity to gold surfaces was investigated in a straightforward fashion by integration of thiol groups. Cysteine (Cys)-free wild-type SP1 (wt SP1) shows no significant affinity to gold surfaces. Therefore, surface accessibility of the SP1 to gold was endowed by introducing Cys residues (using site-directed mutagenesis) as anchoring points at two different sites in the protein structure. In the first variant, Methionine 43, which is located in the protein inner pore, was replaced with a cysteine (mutant name: M43CSP1). In the second variant, Leucine 81, which is located on the protein rim, was replaced with a cysteine (mutant name: L81CSP1). Figure 1 a–c shows the protein structure and the positions of the Cys amino acids in the two mutants. Because SP1 is a dodecamer, each complex presents 12 Cys amino acids, with six on each face of the protein ring. Whilst the Cys thiol groups in M43CSP1 are confined to the inner pore, the L81CSP1 thiol groups are exposed on the outer rim of the protein ring. The two mutants were expressed in *E. coli* and have high stability characteristics (Supporting Information, Figure S1) and complex formation as the wt SP1.[6,7] The position effect of the single-point mutation on the surface binding capability was analyzed by investigating the affinity of the two mutants to ultraflat gold surfaces (roughness less than 5 Å on an area of 5 μm^2).[12]

Dynamic-mode atomic force microscopy (AFM) topographic imaging followed by flooding image analysis[13] (Figure 1 d–f) was used to determine the percentage of the surface covered by the protein. Each of the two gold binding mutants was tested along with the wt SP1 under similar conditions (protein concentration, surface treatment, and deposition time). In flooding analysis, imaged objects which are higher than a predetermined height are shown in the form of the acquired topographic images in brown, whilst surfaces or objects lower than the predetermined height are colored blue. This technique creates a clear contrast between the surface and the investigated object. In the case of SP1, which is 2.5 nm high as observed in our AFM imaging,[8] the threshold was 1.5 nm. The L81CSP1 mutant, which presents thiol groups on the protein rim, covered 98% of the surface (this number may vary by up to 20% owing to tip convolution). The almost complete surface coverage (visualized after scratching the surface in contact mode AFM) is in accordance with the exposed location of the thiol group, thus facilitating its efficient binding to gold. The M43CSP1 mutant, having thiol groups in its inner pore, showed only 60 ± 20% surface coverage, and the wt SP1, with no Cys amino acids, showed almost no binding to the gold surface. Therefore, the

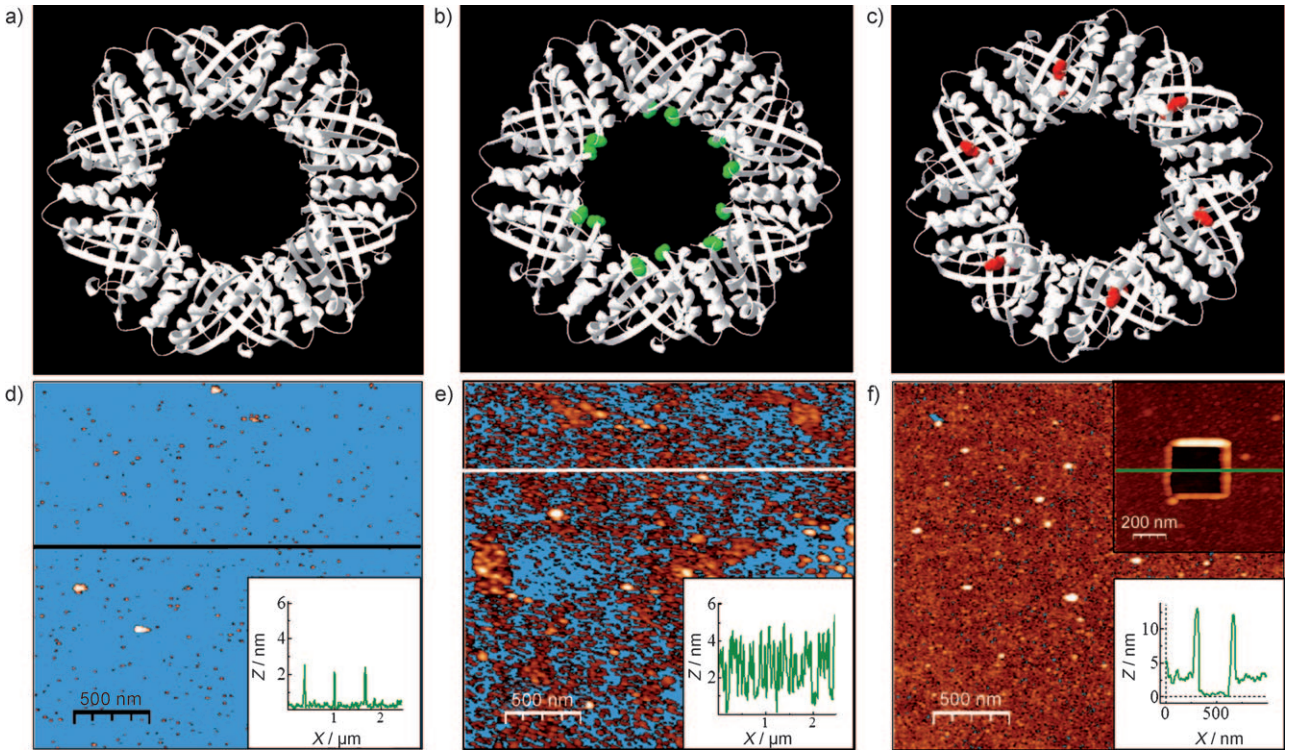

Figure 1. a–c) SP1 mutants (upper; diameter: 11 nm, width: 4 nm) and d–f) the corresponding AFM flooding topography images on an ultraflat gold surface (lower; blue: surface, brown: protein). a,d) wild-type (wt) SP1 (leading to 1.5% surface coverage in (d)), b,e) M43CSP1 mutant presenting thiol groups (green) in the inner pore of the protein (60% surface coverage), and c,f) L81CSP1 mutant presenting thiol groups (red) on the protein outer rim (98% coverage). Insets show the topographic cross-sections of the surface at the marked line. Upper inset in (f) shows the scratched surface with a 2.5 nm-high dense protein layer.

SP1 mutant presenting thiol groups on the outer rim has higher affinity (because of better accessibility) to the gold surface compared to the SP1 mutant with Cys in the inner pore.

As the inner pore was less accessible to the surface, we aimed at controlling the exposure and surface accessibility of the binding peptides by locating them inside the protein ring cavity and controllably releasing them outwards. The SP1 protein complex has twelve N termini facing the inner cavity of the protein, which can be utilized as surface-anchoring points. The mutant M43CSP1 was genetically engineered to present silicon-binding peptides at its inner cavity. The silicon-binding peptide mTBP[14–16] with six amino acids was genetically fused in-frame to the M43CSP1 N termini and expressed in *E. coli*. The resulting protein, named SiSP1, is a ring-shaped homo dodecamer having twelve silica-binding peptides in its inner pore, six on each face of the protein ring. Figure 2 a,b shows the structure of this mutant with retracted and extracted configurations of the binding peptides, respectively.

SiSP1 was expressed in the bacteria-soluble fraction and formed a dodecamer complex with high stability characteristics (Supporting Information, Figure S2 a) and structural motifs as the wt SP1.[4–7] As mentioned above, wt SP1 and its mutants are stable in the presence of chaotropic agents, which denature most proteins. This unique feature was used to control the exposure of the inaccessible peptides in the SiSP1 mutant. Guanidine hydrochloride (GuHCl; a chaotropic

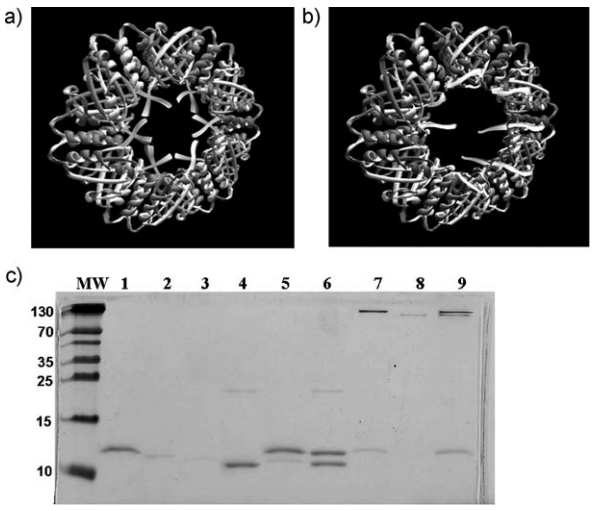

Figure 2. a,b) The SiSP1 mutant in its different estimated conformations a) without GuHCl (N termini retracted) and b) with GuHCl (N termini exposed). c) SDS-PAGE analysis (molecular weights (MW) in kDa) for SiSP1 binding to SiO_2 in the presence of 3 M GuHCl. Lanes 1,2: SiSP1 bound and unbound to SiO_2, respectively; the protein appears only with the precipitated silica. Lanes 3,4: wt SP1 bound and unbound to SiO_2, respectively; the protein does not appear in the precipitated silica. Lanes 5,6: mix (SiSP1 and wt SP1) bound and unbound to SiO_2, respectively; only the mutant binds to silica. Lanes 7–9: bound SiSP1, wt SP1 ,and mix, respectively. Samples 7–9 are not boiled prior to run, showing that the mutant dodecamer specifically binds to the silica as a stable complex while the wt does not.

agent) was used to relax the protein structure without denaturing it, thus facilitating the exposure and surface accessibility of the hidden peptides.

The ability to control the SiSP1 silica-binding was first tested by binding to silica beads (in the presence of GuHCl), followed by SDS-PAGE of the precipitant. The SiSP1 accumulated on the precipitated silica, whereas almost no protein appeared in solution (Figure 2c), indicating that the SiSP1 indeed binds to silica whilst the wt SP1 (appearing in the soluble fraction) does not. To demonstrate the selectivity of the new mutant, the same experiment was conducted with a mixture of SiSP1 and wt SP1: only the silica-binding protein appeared on the precipitated silica beads. Moreover, when the precipitated silica was not boiled prior to SDS-PAGE analysis (conditions that break down the SP1 complex to monomers), the SiSP1 appeared at approximately 120 kDa, as expected, indicating that the whole intact dodecamer complex had bound to the silica. Further verification of the protein complex stability in the presence of GuHCl was conducted using AFM and TEM analysis (Supporting Information, Figure S3).

To characterize the SiSP1 affinity to silica, several comparative binding experiments were conducted by measuring the bound protein concentration for various GuHCl concentrations. Figure 3a,b illustrates the binding of SiSP1 and free mTBP to silica beads. The amount of protein bound to the bead surface clearly depends on the GuHCl concentration. Whilst the free peptides, which are always fully exposed to the silica, bind to it in both the presence and absence of GuHCl (Figure 3a), the SiSP1 protein hardly binds silica in the absence of GuHCl (Figure 3b). An increase in the GuHCl concentration in the solvent is followed by a gradual increase of the bound protein population. This way we control the surface binding of the silica binding mutant. Moreover, the binding curve of the free peptide is linear, whereas a logarithmic fit is observed for the SiSP1 (Figure 3c). The dissociation constants (K_d) for both SiSP1 and the free mTBP were determined by calculating the protein concentration at 50% binding (Figure 3c): a value for K_d of 0.3 μM was determined for SiSP1, and 260 μM for the free peptide (calculations given in detail in the Supporting Information), meaning that when the peptide is presented on the SP1 scaffold, a cooperative effect is observed, and its affinity to the silica increases by three orders of magnitude.

AFM imaging of SiO_2 surfaces provided direct visualization of the protein surface affinity by investigating the surface coverage by various SP1 mutants in the presence or absence of GuHCl. Figure 4 demonstrates the silica surface-binding ability of SiSP1 compared to wt SP1 and the gold binding mutants (M43CSP1 and L81CSP1). In the absence of GuHCl, all of the mutants showed negligible surface coverage in the range 1–7%. Upon addition of 3 M GuHCl, the silica-binding ability of SiSP1 was triggered, and full surface coverage with a SiSP1 monolayer was achieved (Figure 4h), whilst the other mutants did not attach to the surface. The high stability of the SP1 scaffold allows it to expose the hidden peptides at solvent conditions that denature most proteins. Moreover, the use of a chaotropic agent, such as GuHCl, significantly reduces nonspecific binding of the non-silica-binding mutants to the surface (compare Figure 4a–c with Figure 4e–g). The use of a chaotropic agent in this context is an advantage because non-specific binding that may impair device performance could be eliminated.

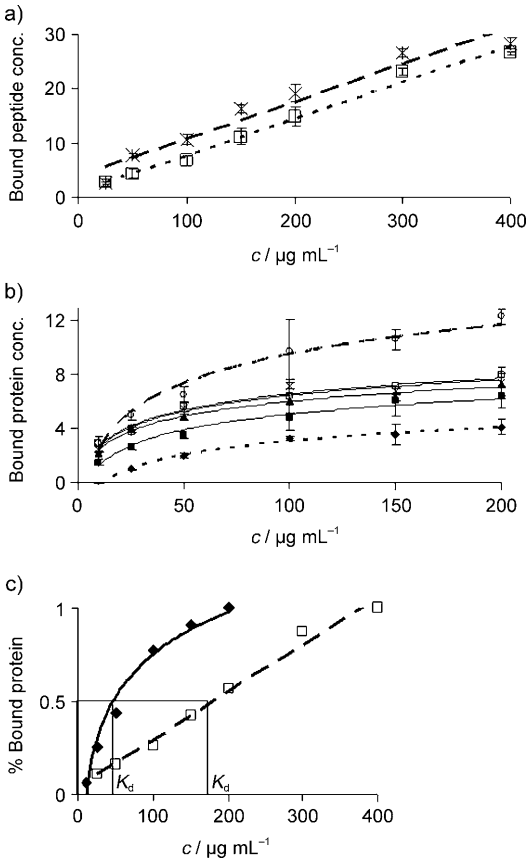

Figure 3. Comparative binding experiments for various GuHCl concentrations. c = total protein concentration given in μmL^{-1}. Bound protein concentrations given in μg peptide per mg of SiO_2. a) mTBP binding: □ peptide with GuHCl, × peptide only. The peptide binds to silica regardless of the change in solvent. b) SiSP1 silica binding in response to GuHCl concentration: ◆ 0 M, ■ 0.1 M, ▲ 0.5 M, × 1 M, □ 2 M, ○ 3 M. c) Dissociation constants of mTBP and SiSP1 binding to SiO_2 in the presence of 3 M GuHCl: ◆ SiSP1 (K_d = 0.3 μM), □ mTBP (K_d = 260 μM).

GuHCl, which in most cases denatures proteins, confers a certain degree of flexibility to the extremely stable SP1 structure, and the N terminals in particular, without denaturing it. This increased flexibility results in an exposure of the silica-binding peptides and facilitates their binding to silica. In a previous work, we showed that SP1 binds Ni-NTA-modified gold nanoparticles (AuNPs) by six His peptides at the N termini in the presence of GuHCl.[8] In that work, incubation with GuHCl led to the formation of GNP-SP1 hybrids. This phenomenon enabled us to demonstrate herein, for the first time, a controllable surface-binding capability of a protein complex simply by changing the solvent conditions.

Protein engineering holds the key to controlling protein–surface interactions. Herein we have described a highly stable protein scaffold that can be engineered to display various moieties that contribute their binding abilities to the protein in a cooperative manner. As previously presented,[8] the SP1

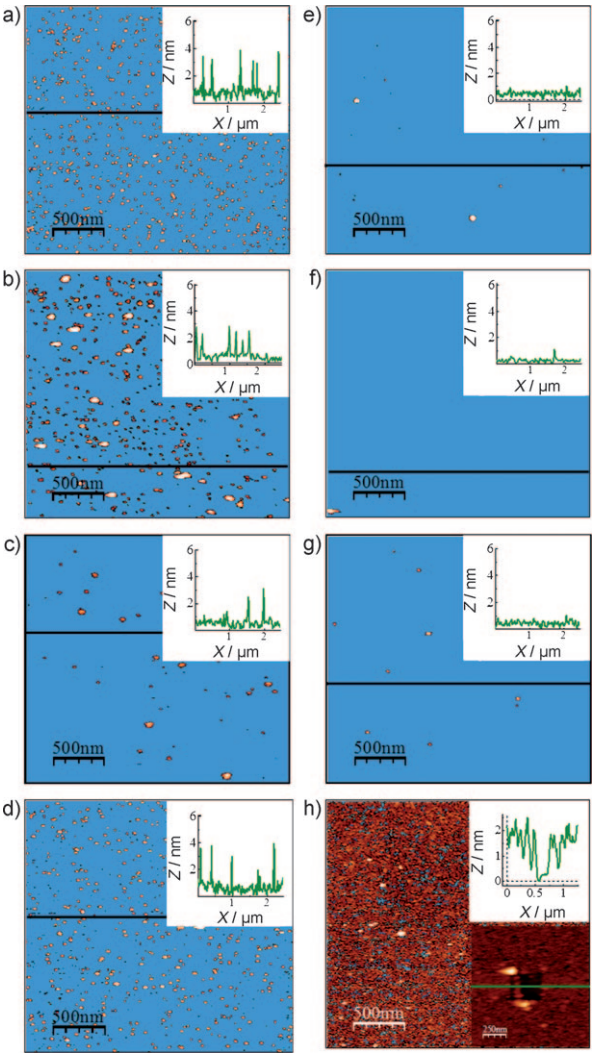

Figure 4. AFM flooding topography images showing the affinity of different SP1 mutants to a SiO_2 surface with or without 3 M GuHCl (blue: surface area, brown: protein). a–d) wt SP1, L81CSP1, M43CSP1, and SiSP1 without GuHCl. All show low nonspecific binding (less than 7% surface coverage) to SiO_2. e–h) wt SP1, L81CSP1, M43CSP1, and SiSP1 with GuHCl. Insets show topographic cross-sections of the surface at the bold line marked on the image. Lower inset in (h) shows the scratched surface where a protein monolayer is observed.

protein is stable upon drying on various surfaces, such as mica or a TEM grid, and its functionality as a molecular scaffold is preserved. Taking advantage of the stability of SP1, its ring-shaped structure, and the location of the N termini in the inner cavity, we were able to selectively and controllably attach SP1 to different surfaces. Moreover, peptides exposure was triggered in a tunable manner under solvent conditions that otherwise reduce nonspecific binding, thus significantly increasing the binding specificity. Overcoming the need for surface modification paves the way for a variety of applications based on protein attachment. The ability to add a switchable binding entity to proteins and utilize its full potential can be of great importance and use for composite materials, biosensors, and nanoelectronic applications.

Experimental Section

E. coli strain DH5α was used for cloning, and *E. coli* strain BL21 (DE3) was used for expression. All bacteria were grown under the same conditions on Luria–Bertani (LB) media at 37 °C on a rotary shaker at 250 rpm. When grown for protein expression, 1 mM isopropyl β-D-thiogalactopyranoside (IPTG) was added to the media at an optical density (O.D.) at 600 nm of 0.8 and the bacteria were grown for a further 4 h, then cells were harvested at 14000 *g* for 15 min.

Both M43CSP1 and L81CSP1 vectors were constructed using site-directed mutagenesis on the ΔNSP1 template previously described in Ref. [6] and performed in accordance to the Stratagene Quickchange protocol with PfuTurbo or deep-vent DNA polymerase. SiSP1 was constructed using two primers with M43CSP1 as the template. For specific primers, see the Supporting Information. All constructs were inserted into pET 29a expression plasmid (Novagen Inc. Madison, WI, USA).

Protein purification and refolding: Cell pellets were resuspended in lysis buffer (50 mM Tris·HCl, 1 mM EDTA, 10 mM $MgCl_2$ pH 8), and sonicated. The insoluble pellets were separated by centrifugation at 14000 *g* for 15 min. Soluble mutated proteins M43CSP1 and SiSP1, were then heat-treated at 85 °C for 30 min. Inclusion bodies of L81CSP1 were washed with IB washing buffer (20 mM Tris·HCl, 2 M urea, pH 8) and then centrifuged at 14000 *g* for 15 min. The pellets were resuspended in denaturation buffer (20 mM Tris·HCl pH 8, 6 M urea, 10 mM dithiothreitol (DTT)) and diluted to a protein concentration of 5 mg mL^{-1}. Denatured proteins were then refolded by dialysis against 20 mM Tris·HCl (pH 7) and 1 mM DTT for 4 days.

A Hitrap Q Sepharose XL ion-exchange FPLC column (1 mL) (Amersham Biosciences, Piscataway, NJ USA), was used to purify the proteins. Samples were loaded on the column using 20 mM piperazine pH 6.3 buffer at a flow rate of 3 mL min^{-1}. Elution was conducted with a gradient of 1 M NaCl in the same buffer and determined at 27–33% salt.

Three different stability analyses were performed on each protein: 1) Heat treatment (85 °C, 30 min); 2) boiling treatment (100 °C, 30 min); 3) Resistance to proteolysis (50 μg mL^{-1} proteinase K, 1 h, 37 °C). Proteinase K activity was quenched by boiling treatment for 5 min. All treatments were followed by centrifugation and analysis by SDS-PAGE.

Silica binding: SiSP1 was mixed with 10 mg silica gel (Aldrich, Steinheim, Germany) in 10 mM MES buffer (pH 6.5), 150 mM NaCl, with or without 3 M GuHCl. The solution was incubated for 1 h on a rotary shaker at room temperature and then the silica was washed three times with the same buffer without GuHCl. Bound protein was analyzed either by SDS-PAGE or by measuring protein concentration using the Micro BCA protein assay kit (Pierce, Rockford, IL, USA). mTBP was synthetically manufactured by BioSight Ltd. (Karmiel, Israel) and was subjected to the above-described tests.

Flat gold surface preparation and deposition procedure: Gold was evaporated (100 nm) on cleaved mica at a rate of 0.5 Å s^{-1} followed by 5 nm of titanium evaporated at 2 Å s^{-1} in a vacuum of over 5×10^{-7} torr. The evaporated samples were heated on a hot plate for 10 to 15 min. Epoxy glue (15 μL, Epo-Tek, Billerica, MA, USA) was used to glue the evaporated gold to a glass surface, which was then heated for 3.5 h at 85 °C followed by overnight cooling. Prior to use, the epoxy sandwich was cleaved using THF solution (99.0% purity; Frutarom, Haifa, Israel), leaving a clean flat gold surface.[12] The sample solution was then deposited on the flat gold surface as on the SiO_2 surfaces.

Surface preparation and binding: Silicon surfaces (0.5 × 0.5 cm) were sonicated in 75 °C heated isopropanol for 20 min, washed with triple distilled water (TDW) and dried under nitrogen. The treated surfaces were plasma-cleaned for 3 min (Femto-Diener Electronic Inc., Nagold, Germany). Samples (5 μL at a final concentration of about 2 mg mL^{-1} protein in 10 mM MES buffer at pH 6.5 with or without 3 M GuHCl) were deposited on the surface directly after the

cleaning procedure, left for 20 seconds, and then gently washed off with TDW and nitrogen-dried.

AFM imaging: A Dulcinea AFM system (NanoTec Electronica, Madrid, Spain) was used under ambient conditions, with Multi75B soft tapping mode AFM tips (Budget Sensor, Sofia, Bulgaria), with a nominal spring constant of 3 $N m^{-1}$, resonance frequency of 60 KHz, and tip apex radius of less than 25 nm. The tip–sample interaction was minimized by using soft AFM tips and low driving amplitudes. All measurements were performed under ambient conditions directly after the deposition. The "scratching" was performed in AFM contact mode with an applied force of about 0.5 μN. WSxM software (NanoTec Electronica, Madrid, Spain) was used to analyze the data.[13]

Received: June 8, 2009
Published online: September 22, 2009

Keywords: nanofabrication · protein structures · self-assembly · SP1 · surface attachment

[1] J. J. Gray, *Curr. Opin. Struct. Biol.* **2004**, *14*, 110.
[2] T. A. Horbett, J. L. Brash, American Chemical Society Meeting, *Proteins at Interfaces II : Fundamentals and Applications*, American Chemical Society, Washington, DC, **1995**.
[3] S. Tang, C. Mao, Y. Liu, D. Q. Kelly, S. K. Banerjee, *IEEE Technical Digest.* **2005**, 181.
[4] O. Dgany, A. Gonzalez, O. Sofer, W. Wang, G. Zolotnitsky, A. Wolf, Y. Shoham, A. Altman, S. G. Wolf, O. Shoseyov, O. Almog, *J. Biol. Chem.* **2004**, *279*, 51516.
[5] W. Wang, O. Dgany, O. Dym, A. Altman, O. Shoseyov, O. Almog, *Acta Crystallogr. Sect. D* **2003**, *59*, 512.
[6] W. X. Wang, O. Dgany, S. G. Wolf, I. Levy, R. Algom, Y. Pouny, A. Wolf, I. Marton, A. Altman, O. Shoseyov, *Biotechnol. Bioeng.* **2006**, *95*, 161.
[7] W.-X. Wang, D. Pelah, T. Alergand, O. Shoseyov, A. Altman, *Plant Physiol.* **2002**, *130*, 865.
[8] I. Medalsy, O. Dgany, M. Sowwan, H. Cohen, A. Yukashevska, S. G. Wolf, A. Wolf, A. Koster, O. Almog, I. Marton, Y. Pouny, A. Altman, O. Shoseyov, D. Porath, *Nano Lett.* **2008**, *8*, 473.
[9] A. Heyman, Y. Barak, J. Caspi, D. B. Wilson, A. Altman, E. A. Bayer, O. Shoseyov, *J. Biotechnol.* **2007**, *131*, 433.
[10] A. Heyman, I. Levy, A. Altman, O. Shoseyov, *Nano Lett.* **2007**, *7*, 1575.
[11] A. Heyman, I. Medalsy, O. Dgany, D. Porath, G. Markovich, O. Shoseyov, *Langmuir* **2009**, *25*, 5226.
[12] P. Wagner, M. Hegner, H.-J. Guentherodt, G. Semenza, *Langmuir* **1995**, *11*, 3867.
[13] I. Horcas, R. Fernandez, J. M. Gomez-Rodriguez, J. Colchero, J. Gomez-Herrero, A. M. Baro, *Rev. Sci. Instrum.* **2007**, *78*, 013705.
[14] K.-I. Sano, H. Sasaki, K. Shiba, *J. Am. Chem. Soc.* **2006**, *128*, 1717.
[15] K.-I. Sano, H. Sasaki, K. Shiba, *Langmuir* **2005**, *21*, 3090.
[16] T. Hayashi, K.-I. Sano, K. Shiba, Y. Kumashiro, K. Iwahori, I. Yamashita, M. Hara, *Nano Lett.* **2006**, *6*, 515.

